Physica Medica 142 (2026) 105712

Contents lists available at ScienceDirect

Physica Medica

journal homepage: www.elsevier.com/locate/ejmp

Effective dose and risk assessment in 18F-FDG PET/CT examinations of lymphoma patients using updated dose coefficients

Forough Jafarian-Dehkordi [a,*], Yazdan Salimi [b], Esmail Jafari [c,d], Majid Assadi [c,d], Christoph Hoeschen [a]

[a] Chair of Medical System Technology, Institute for Medical Technology, Faculty of Electrical Engineering and Information Technology, Otto von Guericke University, Germany
[b] Division of Nuclear Medicine and Molecular Imaging, Geneva University Hospital, CH-1211 Geneva, Switzerland
[c] The Persian Gulf Nuclear Medicine Research Center, Bushehr University of Medical Sciences, Bushehr, Iran
[d] Department of Nuclear Medicine, Molecular Imaging and Theranostics, Bushehr Medical University Hospital, School of Medicine, Bushehr University of Medical Sciences, Bushehr, Iran

ARTICLE INFO

Keywords:
Effective dose
FDG-PET/CT
Radiation risk
Dosimetry
Life time attributable risk

ABSTRACT

Purpose: The objective of this study was to estimate the total effective dose using the updated dose coefficient, and assess the associated cancer risk from radiation exposure in patients undergoing positron emission tomography (PET)/computed tomography (CT) for lymphoma indications.
Methods: This study included 103 patients who underwent FDG-PET/CT. The effective radiation doses to the body was calculated by summing the contribution from internal dosimetry, using the updated dose coefficients based on the ICRP approach, and external dosimetry, using the NCICT software. Based on the effective organ doses and utilizing the risk model introduced in the Biological Effects of Ionizing Radiation VII report, the lifetime attributable risk for cancer incidence (LARCI) and mortality (LARCM) were estimated on an organ-specific basis.
Results: The mean effective dose was 12.4 ± 2.8 mSv (range, 5.1–20.2 mSv), with CT contributing for 74% of the total dose. The LARCI and LARCM values varied by age and sex, with the most pronounced age-related declines observed in the uterus, ovary, and breast for female LARCI (R^2 = 0.83, 0.80, and 0.75, respectively) and in the liver, stomach, and colon for male LARCI (R^2 = 0.71, 0.64, and 0.60, respectively). Similarly, the strongest associations for LARCM were found in the breast, uterus, and ovary for females (R^2 = 0.75, 0.75, and 0.73, respectively) and in the stomach and liver for males (R^2 = 0.66 and 0.63, respectively).
Conclusion: PET/CT scans involve radiation exposure that varies with age and sex, posing higher risks to radiosensitive organs especially at younger ages.

1. Introduction

The integration of positron emission tomography (PET) and computed tomography (CT) in PET/CT systems has revolutionized the field of diagnostic imaging, providing a powerful tool for the detection, staging, and characterization of human diseases, particularly malignant tumors, and the evaluation of treatment responses [1]. While the CT component of PET/CT imaging is based on transmission imaging, capturing X-rays that pass through the body to create anatomical images, the PET component relies on emission imaging, where a radiopharmaceutical highlights metabolic and functional processes [2].

The most widely used positron-emitting radiopharmaceutical in clinical PET/CT imaging is [fluorine-18] 2-fluoro-2-deoxy-D-glucose (18F-FDG), which has a half-life of 109.7 min. This compound is synthesized through radiochemical synthesis in a cyclotron, and decays to stable oxygen-18. 18F-FDG is transported into cells via glucose transporters on the cell membrane and participates in the initial stages of glycolysis, enabling PET imaging to highlight areas of increased metabolic activity, often associated with cancer [3].

Although hybrid PET/CT technology has significantly enhanced diagnostic accuracy, it has also increased patient radiation exposure compared to stand-alone CT or PET scans. This is because the effective

* Corresponding author.
E-mail address: forough.jafarian@ovgu.de (F. Jafarian-Dehkordi).

https://doi.org/10.1016/j.ejmp.2025.105712
Received 4 June 2025; Received in revised form 22 December 2025; Accepted 30 December 2025
Available online 22 January 2026

dose from a PET/CT scan combines the doses from both PET and CT modalities [4]. As a result, the radiological protection for patients undergoing PET/CT scans remains a significant concern. The doses to the patients and corresponding radiation risk from a PET/CT scanner is influenced by several factors such as the type and amount of the imaging protocol, radiopharmaceutical administered, the technical parameters of the CT scan, and the patient's physiological characteristics [5].

Lymphoma is a cancer of the lymphatic system, which is divided into Hodgkin lymphoma (HL), accounting for 10% of cases, and non-Hodgkin lymphoma (NHL), which comprises about 90% of lymphoma cases. Given that lymphoma is a major global health issue with 545,000 new cases diagnosed in 2020, and that many lymphoma patients can live normal lifespans post-treatment, assessing radiation risks in lymphoma patients is crucial [6].

The effective dose, as proposed by the International Commission on Radiological Protection (ICRP), is a widely used metric in medical radiology for risk management and estimating stochastic effects, such as cancer and hereditary effects [7]. It is designed to provide a standardized measure of radiation exposure that accounts for the type of radiation and sensitivity of different tissues to radiation. However, the effective dose does not incorporate age and sex dependencies, which are known to significantly influence radiation risk. This has led to criticism of the concept, as it may not fully capture the true risk for individuals, particularly for younger patients or those undergoing repeated exposures [8]. The Committee on the Biological Effects of Ionizing Radiation (BEIR VII) supports the linear no-threshold (LNT) model for cancer risk at lower doses, suggesting that the risk increases linearly with the radiation dose without threshold [8]. The committee has proposed the concept of the Lifetime Attributable Risk (LAR), which quantifies the probability of the radiation-induced cancer over an individual's lifetime, taking into account age at exposure and sex [9]. This approach provides a more personalized risk assessment, which is particularly relevant for individuals undergoing repeated diagnostic imaging procedures, such as CT and PET scans.

In this study, first, we aim to estimate the effective dose using the recently updated dose coefficients, which are going to be introduced by the ICRP for dosimetry [10]. Unlike the previous ICRP Publication 128, which utilized sex-averaged dose coefficients, these newly proposed coefficients incorporate sex-specific physiological parameters in the dose calculations. These values, derived from a revised bio-kinetic model for 2-[18F]FDG, enhance the dose assessments compared to prior methodologies. The updated model improves evaluating time-integrated activity and organ absorbed dose, addressing key challenges in assessing risks for highly vascularized organs like the lungs and liver. Notably, the updated coefficients demonstrated differences as high as 90% and 44% in time-integrated activity curves for these organs, respectively, compared to earlier approaches [10]. The revised dose coefficients also incorporate an improved representation of urinary excretion dynamics, which enables more accurate estimation of absorbed doses to the bladder wall. This sex-specific approach allows for more individualized dose assessments, representing an evolution in ICRP dosimetric methodology. These advancements provide a robust framework for evaluating organ-specific radiation risks associated with radiopharmaceutical administration. To our knowledge, this study is the first to implement these updated dose coefficients, offering a more precise risk assessment to enhance safety in FDG PET practices.

Using this refined effective dose estimated, we calculate the LAR for cancer incidence (LARCI) and cancer mortality (LARCM) across organs in lymphoma patients undergoing PET/CT scans. By addressing these two objectives, refined dosimetry and individualized organ-based risk modelling, the study aims to advance the characterization of radiation risks in patients undergoing 18F-FDG PET/CT imaging.

2. Materials and methods

2.1. Patient

The present study is a retrospective study involving the examination of FDG-PET/CT scans from 103 adult individuals (53 males and 50 females), with a mean age of 43 years (ranging from 15 to 85 years). They were selected from HL and NHL patients referred to the Persian Gulf nuclear medicine research center in Bushehr, Iran, for whole-body PET/CT. Ethical approval for this study was obtained from the institutional review committee. Before scanning, all patients fasted for a period of at least 6 h and they were permitted to drink only water during this time. An average of 178.6 MBq (ranging from 109.9 to 275.6 MBq) of 18F-FDG was intravenously injected. Following injection, patients were encouraged to consume 1.5 L of water and rest in the dedicated uptake room for about 60 min. Subsequently, patients were instructed to empty their bladder before undergoing the examination. Fasting blood glucose levels were also measured for each patient.

2.2. Scan parameters

The PET/CT studies were performed using a General Electric Discovery IQ PET/CT system. The CT scans were conducted using the following parameters: the slice thickness was set at 3.7 mm, with a pitch of 0.93. The detector was configured to 16 × 0.625 mm, and the beam collimation was 10 mm. The tube voltage was maintained at 120 kV, and the tube current–time product was adjusted automatically for each patient. The time per bed position for PET varied based on the selected protocols, with durations of 1.5, 2, and 2.5 min customized to each patient's need. These variations were influenced by several factors, including the patient's body habitus, clinical indication, and the administered radiotracer dose. For instance, patients with larger body masses or those receiving lower radiotracer doses may require longer acquisition times to ensure a sufficient signal-to-noise ratio and image quality. Similarly, scans focusing on areas with small lesions or subtle tracer uptake may benefit from extended durations to enhance diagnostic precision. Conversely, shorter acquisition times may be suitable for routine studies or when scanner sensitivity is high, enabling faster imaging without compromising quality.

2.3. Dose estimation

Internal dosimetry – To calculate the absorbed dose (D_T) in a specific organ or tissue (T) from the administered activity (A), we used the approach described in ICRP 128 publication [11] as follows:

$$D_T(mGy) = A\Gamma_T^{FDG}$$

In this approach (Γ_T^{FDG}) represents the dose coefficients, which are tabulated by ICRP for different organs, allowing for quick calculations of organ dose from the injected activity. For organs not explicitly listed in the table, they are classified under "other organs," and the corresponding dose coefficient is used for calculations. This allows for the calculation of the absorbed dose for individual organs as well as the entire body. This approach streamlines the dosimetry process in clinical settings. Several research groups have used the values introduced in ICRP publication 128 for this purpose. In the current study, as mentioned earlier, we have used the updated organ dose coefficients for FDG that is given in Table 1 [10].

Using the formula above to calculate the absorbed dose from the administered activity and the formula for calculating equivalent doses H_T for organs based on tissue weighting factors w_T from ICRP publication 103 [12], the effective doses from PET scans, E_{PET}, were calculated as follows:

Table 1
Updated organ dose coefficients for FDG (mGy/MBq) [10].

Organ	Adult male	Adult female
Adrenals	1.4E − 02	1.6E − 02
Brain	3.0E − 02	3.3E − 02
Breast	7.6E − 03	9.7E − 03
Colon wall	1.2E − 02	1.5E − 02
Endosteum	1.0E − 02	1.2E − 02
Extrathoracic region	7.6E − 03	8.5E − 03
Gallbladder wall	1.1E − 02	1.3E − 02
Heart wall	6.5E − 02	8.4E − 02
Kidneys	2.0E − 02	2.3E − 02
Liver	1.5E − 02	1.8E − 02
Lungs	1.3E − 02	1.7E − 02
Lymphatic nodes	1.3E − 02	1.4E − 02
Muscle	8.3E − 03	1.0E − 02
Oesophagus	1.5E − 02	1.7E − 02
Oral mucosa	8.8E − 03	9.9E − 03
Ovaries	–-	2.4E − 02
Pancreas	1.6E − 02	1.8E − 02
Prostate	2.7E − 02	––
Red bone marrow	1.5E − 02	1.8E − 02
Salivary glands	7.8E − 03	9.7E − 03
Skin	6.3E − 03	7.7E − 03
Small intestine wall	1.3E − 02	1.7E − 02
Spleen	1.4E − 02	1.7E − 02
Stomach wall	1.2E − 02	1.3E − 02
Testes	8.6E − 03	–-
Thymus	9.8E − 03	1.2E − 02
Thyroid	9.1E − 03	1.1E − 02
Urinary bladder wall	7.5E − 02	9.2E − 02
Uterus/cervix	–	3.3E − 02

$$E(mSv) = \sum_T w_T.H_T = A\sum_T w_T.\Gamma_T^{FDG}$$

External dosimetry − A tube voltage of 120 kVp was kept constant for all patients. The CT acquisition parameters including kVp, tube current (ranging from 220 mA to 330 mA based on patient weight), CTDI vol (32 cm phantom), and pitch factor as well as patient information including age, gender, height, and weight were extracted from the DICOM header information. For all patients, the scan range for CT was set to a whole-body scan.

We used pre-tabulated Monte Carlo (MC) based NCI software for dose calculations. Although there are differences between the pre-tabulated methods and patient-specific MC simulations, our method accounts for patient body habitus in term of weight and height as well as CT beam parameters such as kVp, bringing it one step closer to personalized patient-specific dosimetry [13,14].

These data were then used with the NCICT (National Cancer Institute dosimetry system for CT) Monte-Carlo pre-tabulated software [15] to calculate the organ doses and effective doses from the CT scan for patients. The calculation was based on the phantom selected from the NCI library according to patient information. To achieve this, NCICT integrates several advanced technologies, such as a library of advanced computational human models, detailed x-ray simulations from a reference CT scanner, and an intuitive graphical interface [16].

Finally, the effective doses from [^{18}F-FDG] PET/CT imaging were calculated by summing the effective doses from the PET and CT components as follows:

$$E = E_{CT} + E_{PET}$$

2.4. Radiation risk estimation

In this study we used the method introduced in the BEIR VII report to estimate the radiation-induced cancer risk in the form of LAR [9] in thyroid, stomach, colon, liver, lung, prostate, breast, uterus, ovary, and bladder. This parameter represents the number of additional cancer cases in an irradiated group compared to a non-irradiated group and is used for estimating all cancers including solid cancers and leukemia.

We collected the LAR values from tables 12D-1 and 12D-2 from the BEIR VII report. For patients whose ages were not explicitly listed in the tables, their values were estimated using linear interpolation between the two closest age groups. It should be noted that, according to these tables, the pediatric age group is defined as below 15 years. Therefore, all our patients were considered adults. Using the interpolated LAR values, the risk R was calculated individually for each patient and organ with the following equation:

$$R = \sum_T r_T.H_T$$

Where r_T represents the LAR values per unit of equivalent dose H received by the tissue T [8].

3. Results

The effective doses for male and female patients were calculated, yielding mean values of 12.0 ± 2.7 mSv for males and 12.7 ± 2.9 mSv for females. The distribution of effective dose values across different BMI categories is illustrated in Fig. 1. As depicted in the figure, the CT component constitutes the predominant portion of the total dose across all BMI groups, with a 74% contribution in the mean effective dose. The mean dose-length product (DLP) and volume CT dose index (CTDIvol) in the study were 1175.04 mGy·cm and 7.24 mGy, respectively. Pearson correlation analysis revealed a strong positive correlation between PET/CT effective dose and patient body mass ($P < 0.05$; $R^2 = 0.94$ for males and $R^2 = 0.73$ for females), attributable to the weight-based adjustment of administered activity and CT scan parameters. Furthermore, multiple regression analysis indicated no statistically significant gender-based difference in effective dose when patient weight was accounted for.

Figs. 2, 3, 4, and 5 illustrate the LARCI and LARCM values for body organs following a single PET/CT examination. As evident from the figures, age plays a crucial role in both LARCI and LARCM. For female LARCI values, the strongest associations with age-related decline were observed in the uterus ($R^2 = 0.83$), ovary ($R^2 = 0.80$), and breast ($R^2 = 0.75$). Moderate associations were found in the stomach ($R^2 = 0.59$) and lung ($R^2 = 0.54$). Similarly, for female LARCM values, the breast ($R^2 = 0.75$), uterus ($R^2 = 0.75$), and ovary ($R^2 = 0.73$) demonstrated the strongest associations, while the bladder ($R^2 = 0.52$) and lung ($R^2 = 0.52$) showed moderate associations. In male patients, LARCI values showed the strongest associations in the liver ($R^2 = 0.71$), stomach ($R^2 = 0.64$), and colon ($R^2 = 0.60$), while moderate associations were observed in the thyroid ($R^2 = 0.54$) and bladder ($R^2 = 0.56$). For male LARCM values, the strongest associations were observed in the stomach ($R^2 = 0.66$) and liver ($R^2 = 0.63$), with weaker associations for the bladder ($R^2 = 0.29$). The prostate showed a negligible association for

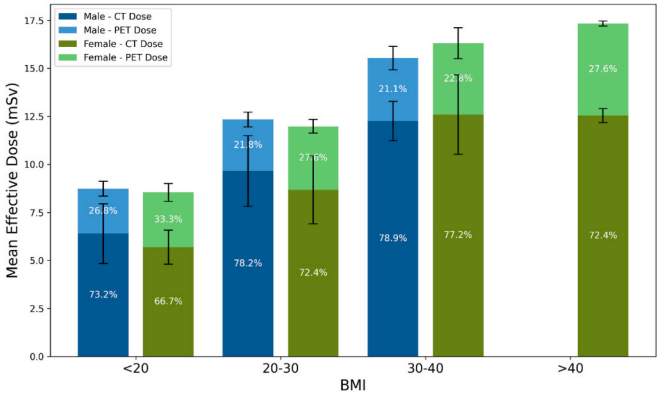

Fig. 1. Mean effective doses from CT and PET scans in PET/CT examinations of lymphoma patients, categorized by BMI (Note that only female patients had BMI > 40).

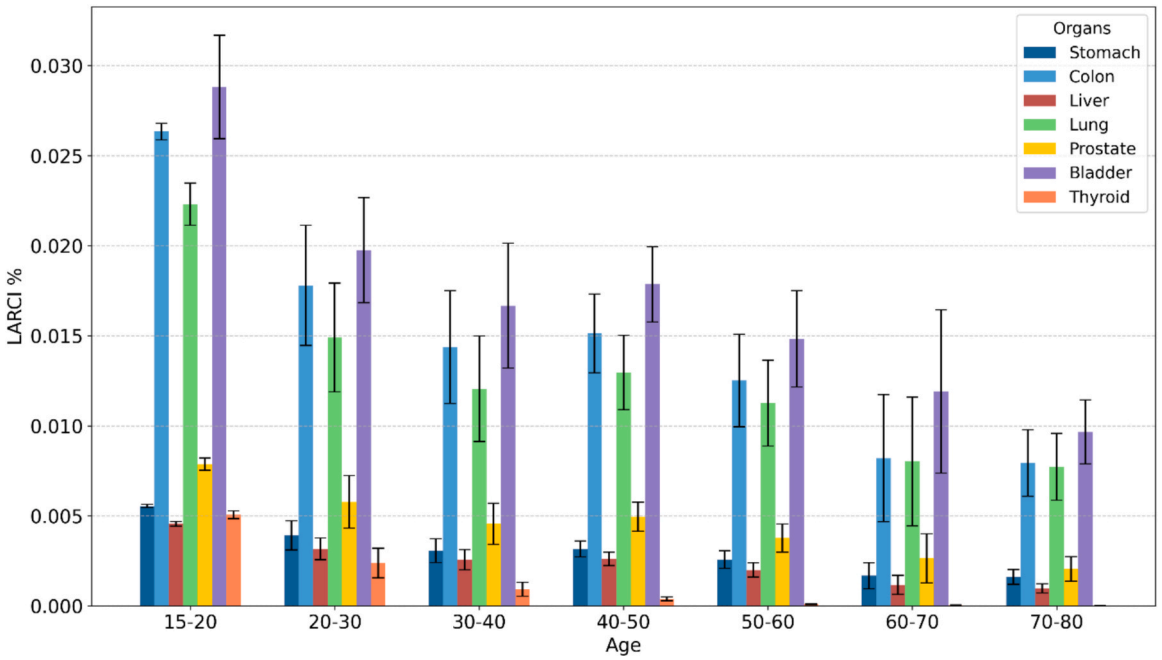

Fig. 2. Life-Attributable Risk of Cancer Incidence (LARCI) from FDG PET/CT scans for male patients, categorized by age.

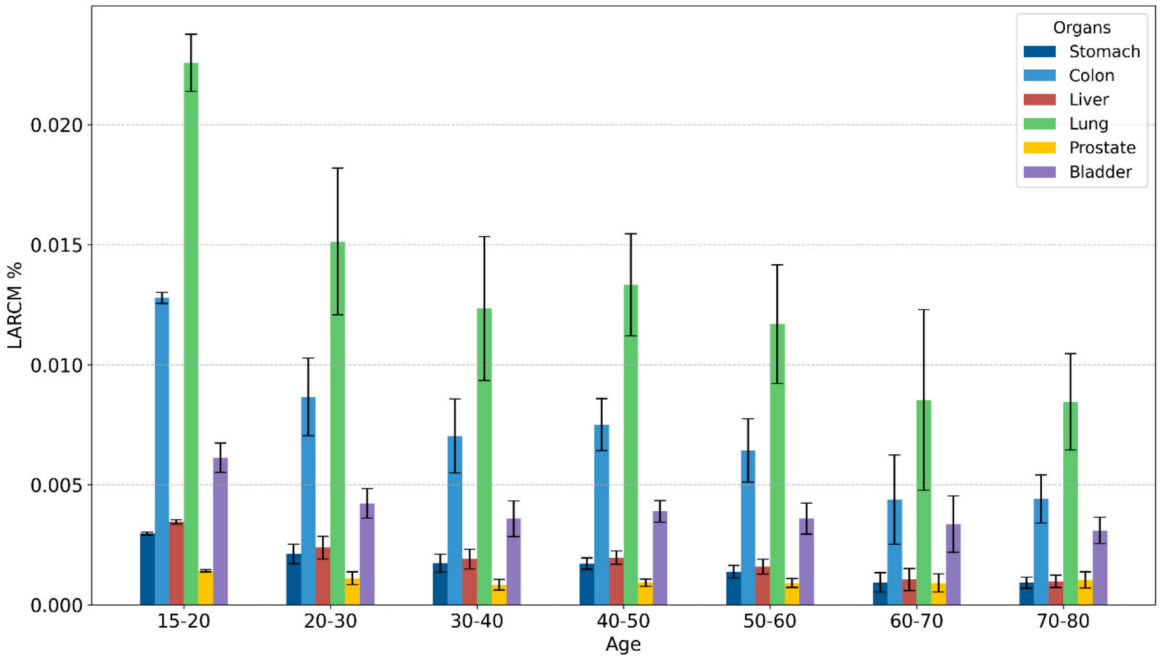

Fig. 3. Life-Attributable Risk of Cancer Mortality (LARCM) from FDG PET/CT scans for male patients, categorized by age.

LARCM ($R^2 = 0.07$, $p > 0.05$) and moderate association for LARCI ($R^2 = 0.59$).

4. Discussion

The potential risk associated with radiation exposure is an essential consideration in evaluating PET/CT scanning in clinical practice. Accurately quantifying and understanding this radiation risk is crucial for assessing the risk–benefit ratio of the procedure and moving towards safer procedure for patients. This personalized measurement can be useful for both the justification and optimization steps.

One common way to quantify the risk is to use the effective dose which provides a metric to relate radiation exposure to the potential radiation-induced risk by accounting for tissue and organ sensitivities and the biological effectiveness of different ionizing radiations. This allows for a comparative analysis of the radiation-induced risks from the radiopharmaceutical and the x-ray components of the PET/CT scan. For calculating the organ dose from 18F-FDG, we used new dose coefficients that are going to be published in the revised version of the ICRP publication 128. While several studies have addressed the calculation of LARCI and LARCM for PET/CT, to our knowledge, this is the first to apply the recently proposed coefficients for this purpose.

The effective dose for the lymphoma patients undergoing PET/CT in this study was 12.4 ± 2.8 mSv. The effective dose increased with the

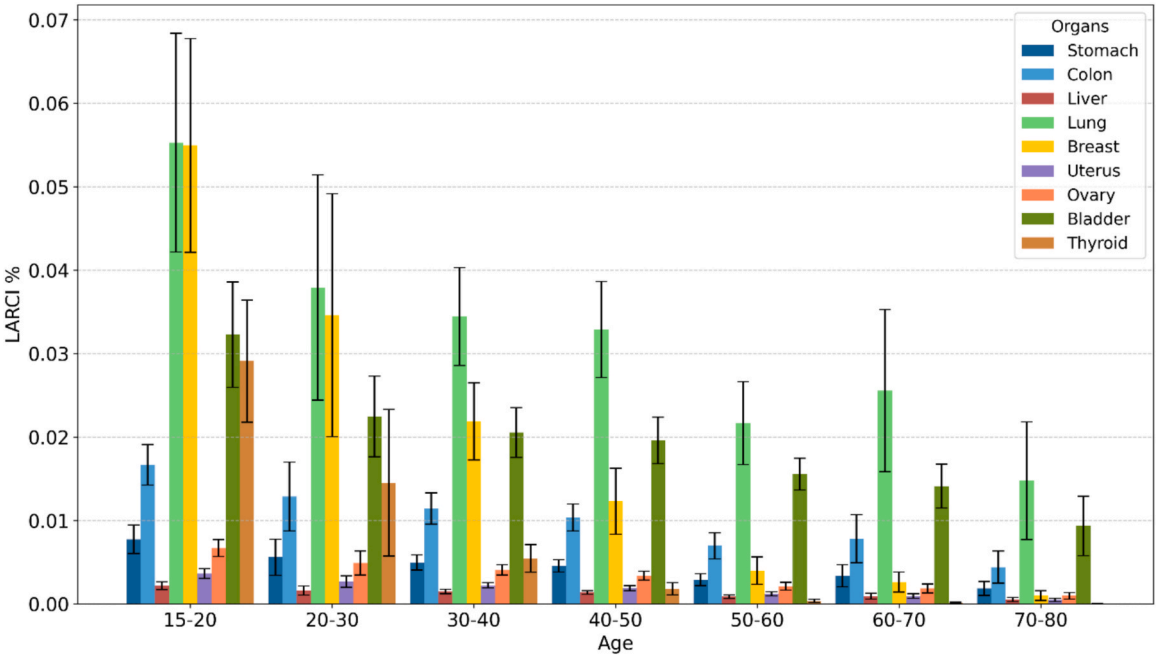

Fig. 4. Life-Attributable Risk of Cancer Incidence (LARCI) from PET/CT scans for female patients, categorized by age.

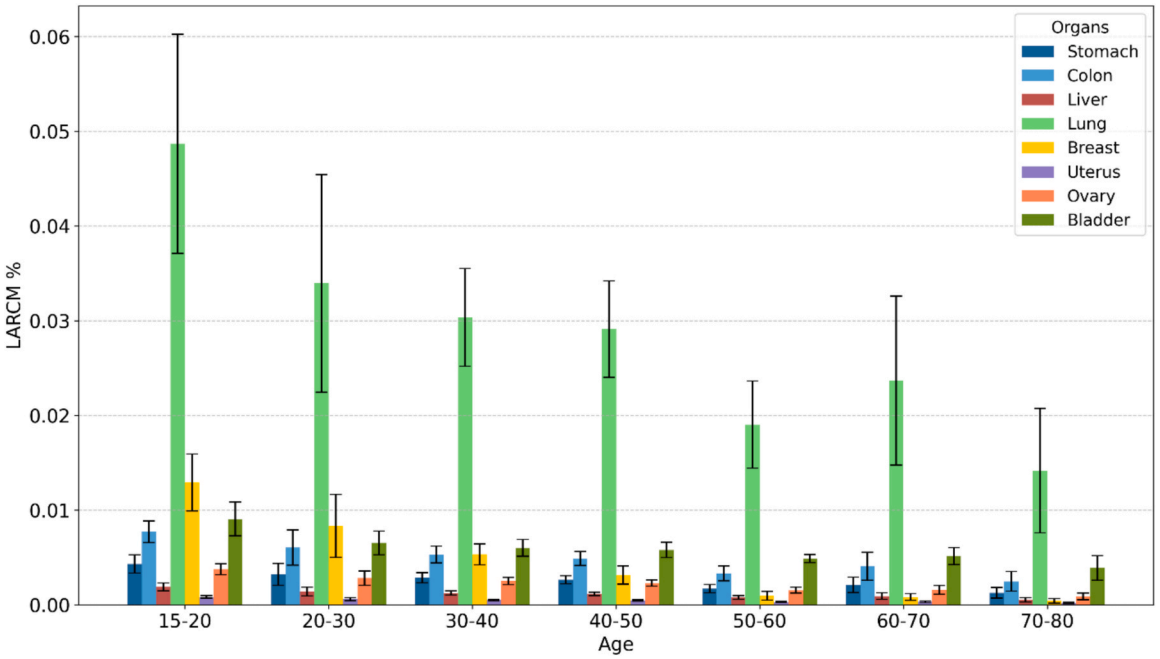

Fig. 5. Life-Attributable Risk of Cancer Mortality (LARCM) from PET/CT scans for female patients, categorized by age.

patient's body mass and showed a strong correlation. The maximum effective dose was 17.5 mSv (3.6 mSv from PET and 13.9 mSv from CT) in a patient with a BMI of 26.8. To put this into perspective, this value is more than 7 times higher than the annual global background radiation of 2.4 mSv. Although this effective dose didn't belong to the highest BMI, the patient who had the highest BMI had comparable effective dose of 16.2 mSv. For comparison, the minimum effective dose was 5.6 mSv which was for the patient with the BMI of 15.2. This correlation between effective dose from PET/CT and BMI can be of concern, especially those with high BMIs.

The calculated effective dose in this study is in close agreement with the values observed by Mahmud et al. and Paiva et al. where they reported effective doses of 13.8 and 16.0 mSv for their patients, respectively [17,18]. There were, however, some studies who reported values either lower or higher than our observations. For example, Quinn et al. and Kessara et al. reported effective doses of respectively 24.4 mSv and 20.5 mSv [19,20], and Saleh et al. calculated effective dose of 8.2 ± 1.3 mSv for their lymphoma patients who underwent FDG PET scan [21]. This variation in the effective dose reported by different groups can be attributed to several parameters as follows:

Dose from the CT can be influenced by the scanner type and scanning protocol. For instance, a study showed that the dose index for multi-slice CT scanners is generally about 34% higher than that of single-slice scanners, though newer multi-slice models may incorporate dose

reduction technologies [22,23]. As shown in another study, the number of detector rows also influences the effective dose, with 64-detector row CT systems averaging 7.5 mSv for comprehensive stroke imaging, whereas 320-detector row CT systems deliver approximately 10.6 mSv for the same protocol [24]. Scanner settings and protocols are the most significant drivers of dose variation, as technical parameters such as X-ray tube settings and scan area can differ widely between institutions leading to different CTDIvol [25].

Another set of parameters affecting effective dose in PET/CT imaging are factors related to functional imaging. Patient-specific parameters such as body mass index and blood glucose, together with the institutional protocols, and scanner technology are among the factors that may affected the activity administered by a factor of more than five and consequently affect the absorbed dose [26].

Of the total effective dose our patients received, CT accounted for 74% of the dose, which is close to the 73% and 73.5% reported by Salah et , and Brix et , respectively [21,27]. Higher radiation dose from the CT component, which is the result of enhanced setting to acquire good quality anatomical images, explains the higher contribution of CT to the effective dose and cancer risks [28].

The effective dose has been successfully used to compare the relative risks of different radiation exposures. However, to account for factors beyond absorbed dose and tissue radio-sensitivity, LAR can be used, as recommended in the BEIR VII report [29–31]. LAR represents the likelihood that an individual will develop or die from cancer due to radiation exposure, referred to as LARCI and LARCM, respectively [9]. The LAR values are expected to have a negative correlation with age, which is explained by the fact that radio-sensitivity of organs is higher at younger ages [9,32–34]. In line with other studies, the result of our analysis also highlighted a clear age-dependent decline in LARCI and LARCM across multiple organs, with notable sex-specific differences.

In females, reproductive and glandular tissues, namely the uterus, ovary, and breast, exhibited the strongest association with aging, reflecting their change of radio-sensitivity and biological vulnerability over time. For male patients, the liver and stomach demonstrated more pronounced correlations with age, suggesting that metabolic and digestive tissues are heavily influenced by age-related physiological changes that affect radiation-induced risk. The weaker associations observed for the prostate and bladder underscore important tissue-specific aging processes and variations in radiation sensitivity. These observations underline importance of organ- and sex-specific approaches to dose–response evaluations in nuclear medicine. These findings are consistent with observations reported in similar investigations which have likewise demonstrated that sex hormones, cellular proliferation rates, and endocrine factors can alter tissue responsiveness to radiation over a lifetime [35]. Immunological and hormonal differences between males and females are responsible for the different responses observed between the sexes [36].

The pronounced age dependence in the uterus, ovary, and breast in females and liver and stomach in males underscores potential vulnerability in younger female patients, suggesting a greater need for dose optimization in reproductive tissues. By integrating organ-specific coefficients that reflect both sex and age, nuclear medicine practitioners can move closer to precision dosimetry, thereby improving patient safety and treatment efficacy.

Building on these findings, it is important to acknowledge that the primary limitation of this study is the use of LAR values from the BEIR VII report, which are based on U.S. population data. These values may require adjustment when applied to a different population with distinct demographic and geographic characteristics. To enhance the accuracy of radiation risk assessment, future research should incorporate cancer incidence rates specific to the Iranian population, providing a more representative baseline and refined LAR estimates. Another limitation is the relatively small sample size, which may impact the statistical strength of the correlation between organ-specific LAR and age. To improve the reliability of these findings and better assess age-related variations in radiation risk, future studies should include a larger and more diverse population.

5. Conclusions

In this study, within SINFONIA which was an EU-funded project entitled radiation risk appraisal for detrimental effects from medical exposure during management of patients with lymphoma or brain tumor, the effective dose and associated radiation risk in lymphoma patients undergoing 18F-FDG PET/CT examinations were estimated using recently updated dose coefficients. In the context of this European project, the study addresses the need for improved assessment of cumulative radiation exposure from repeatedly performed diagnostic imaging in a sensitive patient population. By providing quantitative estimates of patient dose from PET/CT, a modality widely used in lymphoma staging, response assessment, and follow-up, the study supports SINFONIA's objective of reinforced medical exposure risk appraisal and contributes reference data for patient-centered dosimetry, uncertainty evaluation, and future dose optimization strategies within integrated imaging and therapy pathways. This work is consistent with other investigations in this project [37–39] that use quantitative dose data to support radiation protection and risk appraisal across different clinical exposure scenarios.

PET/CT scanning provides significant diagnostic and therapeutic insights, but it also imposes a radiation dose that should not be overlooked, particularly for younger or overweight patients who may be more susceptible to long-term adverse effects. Our findings indicate variability across effective dose measurements, driven by factors such as administered activity, CT protocols, technology of the scanner, and pathology types. Moreover, the CT component was frequently the dominant contributor to the total effective dose.

This study shows that LARCI and LARCM values vary with age and sex, with younger individuals and women facing higher risks. These observations highlight the need for personalized radiation protection strategies, where the sex, age, and clinical status of each patient inform decision-making regarding scan protocols and follow-up intervals.

The results reported in this study were from single PET/CT scans. As cancer patients often undergo multiple radiological studies, clinicians, radiologists, and medical physicists must remain attentive to cumulative doses. Larger-scale, prospective investigations will be instrumental in validating our findings, guiding the development of evidence-based surveillance protocols, and minimizing secondary cancer risks. Ultimately, a comprehensive understanding of both the benefits and risks of PET/CT scans will support efforts to optimize patient care, ensuring that diagnostic and therapeutic objectives are met while limiting unnecessary radiation exposure. This integrated approach to risk–benefit assessment is especially relevant for vulnerable populations, thereby enhancing patient safety and outcomes in nuclear medicine practice.

Declaration of competing interest

The authors declare that they have no known competing financial interests or personal relationships that could have appeared to influence the work reported in this paper.

Acknowledgement

This study was partially funded by the Euratom research and training programme 2019-2020 through the SINFONIA project, grant agreement No. 945196.

References

[1] Alkhorayef M. Effective radiation doses in pediatric PET/CT examinations: pilot study. Appl Radiat Isot 2021;168:109412. https://doi.org/10.1016/j.apradiso.2020.109412.

[2] Townsend DW. Multimodality imaging of structure and function. Phys Med Biol 2008;53:R1–39. https://doi.org/10.1088/0031-9155/53/4/R01.

[3] Hays MT, Watson EE, Thomas SR, Stabin M. MIRD dose estimate report no. 19: radiation absorbed dose estimates from (18)F-FDG. J Nucl Med 2002; 43(2): 210–4 , [https://doi.org/Review][PMID: 11850487].

[4] 1990 Recommendations of the International Commission on Radiological Protection. Ann ICRP. 1991;21:1–201.

[5] International Commission on Radiological Protection. Radiation dose to patients from radiopharmaceuticals: A report of Committee 3 adopted by the International Commission on Radiological Protection. Annals of the ICRP. 1991;22(3):i. doi: 10.1016/0146-6453(91)90017-B.

[6] Sung H, Ferlay J, Siegel RL, Laversanne M, Soerjomataram I, Jemal A, et al. Global cancer statistics 2020: GLOBOCAN estimates of incidence and mortality worldwide for 36 cancers in 185 countries. CA Cancer J Clin 2021;71:209–49. https://doi.org/10.3322/caac.21660.

[7] Harrison J, Day P. Radiation doses and risks from internal emitters. J Radiol Prot 2008;28:137–59. https://doi.org/10.1088/0952-4746/28/2/R01.

[8] Brenner DJ. We can do better than effective dose for estimating or comparing low-dose radiation risks. Ann ICRP 2012;41:124–8. https://doi.org/10.1016/j.icrp.2012.07.001.

[9] Health Risks from Exposure to Low Levels of Ionizing Radiation: BEIR VII Phase 2. Washington, D.C.: National Academies Press; 2006.

[10] Kamp A, Andersson M, Leide-Svegborn S, Noβke D, Mattsson S, Giussani A. A revised compartmental model for biokinetics and dosimetry of 2-18FFDG. EJNMMI Phys 2023;10:10. https://doi.org/10.1186/s40658-023-00528-9.

[11] Mattsson S, Johansson L, Leide Svegborn S, Liniecki J, Noßke D, Riklund KÅ, et al. Radiation dose to patients from radiopharmaceuticals: a compendium of current information related to frequently used substances. Ann ICRP 2015;44:7–321. https://doi.org/10.1177/0146645314558019.

[12] Valentin J. The 2007 recommendations of the international commission on radiological protection. ICRP publication 103. Ann ICRP 2007;37(2–4):1–332. https://doi.org/10.1016/j.icrp.2007.10.003.

[13] Akhavanallaf A, Fayad H, Salimi Y, Aly A, Kharita H, Al Naemi H, et al. An update on computational anthropomorphic anatomical models. Digit Health 2022;8: 20552076221111941. https://doi.org/10.1177/20552076221111941.

[14] Salimi Y, Akhavanallaf A, Mansouri Z, Shiri I, Zaidi H. Real-time, acquisition parameter-free voxel-wise patient-specific Monte Carlo dose reconstruction in whole-body CT scanning using deep neural networks. Eur Radiol 2023;33: 9411–24. https://doi.org/10.1007/s00330-023-09839-y.

[15] Lee C, Kim KP, Bolch WE, Moroz BE, Folio L. NCICT: a computational solution to estimate organ doses for pediatric and adult patients undergoing CT scans. J Radiol Prot 2015;35:891–909. https://doi.org/10.1088/0952-4746/35/4/891.

[16] Lee C, Yeom YS, Folio L. CT organ dose calculator size adaptive for pediatric and adult patients. Biomed Phys Eng Express 2022. https://doi.org/10.1088/2057-1976/ac9845.

[17] Mahmud MH, Nordin AJ, Saad FFA, Azman AZF. Estimation of patient radiation dose from whole body 18 F- FDG PET/CT examination in cancer imaging: a preliminary study. J Phys Conf Ser 2014;546:12008. https://doi.org/10.1088/1742-6596/546/1/012008.

[18] Paiva FG, do Carmo Santana P, Mourão AP. Evaluation of patient effective dose in a PET/CT test. Appl Radiat Isot 2019;145:137–41. https://doi.org/10.1016/j.apradiso.2018.12.024.

[19] Kessara A, Buyukcizmeci N, Gedik GK. Estimation of patient organ and whole-body doses in 18F-FDG PET/CT scan. Radiat Prot Dosim 2023;199:61–8. https://doi.org/10.1093/rpd/ncac218.

[20] Quinn B, Dauer Z, Pandit-Taskar N, Schoder H, Dauer LT. Radiation dosimetry of 18F-FDG PET/CT: incorporating exam-specific parameters in dose estimates. BMC Med Imaging 2016;16:41. https://doi.org/10.1186/s12880-016-0143-y.

[21] Salah H, Mayhoub FH, Sulieman A, Abuzaid M, Al-Mohammed HI, Alkhorayef M, et al. Fluoro-D-glucose (18F-FDG) PET/CT and patient effective dose. Radiat Phys Chem 2020;173:108926. https://doi.org/10.1016/j.radphyschem.2020.108926.

[22] Moro L, Bolsi A, Baldi M, Bertoli G, Fantinato D. Tomografia computerizzata a strato singolo e a strato multiplo: confronto dosimetrico con i livelli diagnostici di riferimento [Single-slice and multi-slice computerized tomography: dosimetric comparison with diagnostic reference dose levels]. Radiol Med 2001;102:262–5.

[23] Brix G, Nagel HD, Stamm G, Veit R, Lechel U, Griebel J, et al. Radiation exposure in multi-slice versus single-slice spiral CT: results of a nationwide survey. Eur Radiol 2003;13:1979–91. https://doi.org/10.1007/s00330-003-1883-y.

[24] Diekmann S, Siebert E, Juran R, Roll M, Deeg W, Bauknecht H-C, et al. Dose exposure of patients undergoing comprehensive stroke imaging by multidetector-row CT: comparison of 320-detector row and 64-detector row CT scanners. AJNR Am J Neuroradiol 2010;31:1003–9. https://doi.org/10.3174/ajnr.A1971.

[25] Curran T-I, Maher M, McLaughlin P, Coffey F, O'Neill S. Analysis of effective dose at computed tomography in a modern 64 slice multidetector CT. System in an Irish Tertiary Care Centre with Local and International Reference Standards. 2020.

[26] Kwon HW, Kim JP, Lee HJ, Paeng JC, Lee JS, Cheon GJ, et al. Radiation dose from whole-body F-18 fluorodeoxyglucose positron emission tomography/computed tomography: nationwide survey in Korea. J Korean Med Sci 2016;31(Suppl 1): S69–74. https://doi.org/10.3346/jkms.2016.31.S1.S69.

[27] Brix G, Lechel U, Glatting G, et al. Radiation exposure of patients undergoing whole-body dual-modality 18F-FDG PET/CT examinations. J Nucl Med 2005;46 (4):608–13 [https://doi.org/Study] [PMID: 15809483].

[28] Huang B, Law M-W-M, Khong P-L. Whole-body PET/CT scanning: estimation of radiation dose and cancer risk. Radiology 2009;251:166–74. https://doi.org/10.1148/radiol.2511081300.

[29] Recommendations of the International Commission on Radiological Protection adopted by the Commission in November 1990. Oxford, New York [et autres]: Pergamon; 1991.

[30] United Nations Scientific Committee on the Effects of Atomic Radiation (UNSCEAR), New York, NY (United States). Sources and effects of ionizing radiation. UNSCEAR 2000 report to the General Assembly, with scientific annexes. Volume I: Sources. UN; 2000. doi:10.18356/49c437f9-en.

[31] Boice Jr JD. The linear nonthreshold (LNT) model as used in radiation protection: an NCRP update. Int J Radiat Biol 2017;93(10):1079–92. https://doi.org/10.1080/09553002.2017.1328750.

[32] Wen JC, Sai V, Straatsma BR, McCannel TA. Radiation-related cancer risk associated with surveillance imaging for metastasis from choroidal melanoma. JAMA Ophthalmol 2013;131:56–61. https://doi.org/10.1001/jamaophthalmol.2013.564.

[33] Ivanov VK, Kashcheev VV, Chekin SY, Maksioutov MA, Tumanov KA, Vlasov OK, et al. Radiation-epidemiological studies of thyroid cancer incidence in Russia after the Chernobyl accident (estimation of radiation risks, 1991-2008 follow-up period). Radiat Prot Dosim 2012;151:489–99. https://doi.org/10.1093/rpd/ncs019.

[34] Land CE, Tokunaga M, Koyama K, Soda M, Preston DL, Nishimori I, et al. Incidence of female breast cancer among atomic bomb survivors, Hiroshima and Nagasaki, 1950-1990. Radiat Res 2003;160:707–17. https://doi.org/10.1667/rr3082.

[35] Narendran N, Luzhna L, Kovalchuk O. Sex difference of radiation response in occupational and accidental exposure. Front Genet 2019;10:260. https://doi.org/10.3389/fgene.2019.00260.

[36] Stricklin D, Millage K. Evaluation of demographic factors that influence acute radiation response. Health Phys 2012;103(2):210–6. https://doi.org/10.1097/HP.0b013e31824.

[37] Romanyukha A, Mazloumi M, de Waelheyns T, Mishra N, Jacobs J, Fitousi N. Development of a context-aware integrated training module based on large language models for continuous education in radiation protection. Phys Med 2025; 137:105090. https://doi.org/10.1016/j.ejmp.2025.105090.

[38] Salimi Y, Shiri I, Mansouri Z, Zaidi H. Development and validation of fully automated robust deep learning models for multi-organ segmentation from whole-body CT images. Phys Med 2025;130:104911. https://doi.org/10.1016/j.ejmp.2025.104911.

[39] de Saint-Hubert M, Romero-Expósito M, Liszka M, van Hoey O, Pinasti S, Eliasson L, et al. Radiation protection in proton therapy: Insights from a multi-institutional survey and experimental measurements within the SINFONIA project. Phys Med 2025;137:105049. https://doi.org/10.1016/j.ejmp.2025.105049.